sample then gives

$$j(t)=\int_0^1 j_c(x,t)dx-(d/dt)\omega(t). \quad \text{(A2)}$$

The potential, $V(t')$ is given by

$$V(t')=V_0-(1/C_d)\int_0^{t'} J(t')dt'. \quad \text{(A3)}$$

Converting the right side of this expression to dimensionless quantities by the prescription of Eqs. (8), one obtains

$$\omega(t)=(C_s/C_d)\int_0^t j(t)dt. \quad \text{(A4)}$$

Equation (A2) for the current can now be written

$$j(t)=\chi\int_0^1 j_c(x,t)dx, \quad \chi=C_d/(C_s+C_d), \quad \text{(A5)}$$

which replaces Eq. (17). The rest of the analysis is unchanged.

PHYSICAL REVIEW VOLUME 159, NUMBER 3 15 JULY 1967

Trapping Processes in Amorphous Selenium*

R. M. BLAKNEY†
Institute of Optics, University of Rochester, Rochester, New York

AND

H. P. GRUNWALD‡
Department of Physics, University of Rochester, Rochester, New York

(Received 15 December 1966)

The theory of small-signal current transients is applied to the study of electron trapping processes in amorphous selenium. In the experiment, a 10^{-8}-sec light pulse illuminated one side of the sample and produced free carriers near this surface. The free electrons were drawn across the sample in an applied electric field, and the shape of the current transients thus produced was studied. The shape of these transients indicated that electron trapping processes in vitreous selenium involve three distinct species of trap: those which control the mobility (m traps), a deep trapping level (d traps), and a shallow trapping level (s traps). Magnitudes are given for the ratio of the m-trap density to the density of states in the conduction band (N_m/N_c) and for the ratio of the s-trap density to the density of states in the conduction band (N_s/N_c). For a selenium film which has been evaporated onto a substrate held at 38°C during the evaporation, these ratios are $N_m/N_c=5.2\times10^{-4}$ and $N_s/N_c=2.4\times10^{-6}$, respectively. It is further shown that the magnitude of these ratios decreases as the substrate temperature at which the samples are prepared is increased. The energy separation of the s level and the m level from the conduction-band edge depends also on the sample preparation, the separation increasing as the substrate temperature is increased. For the film prepared at 38°C, the levels are at $E_s=0.39$ eV and $E_m=0.29$ eV, respectively, below the conduction-band edge. The capture probability for both the s and d traps was measured and was found to increase exponentially with $1/T$ with a characteristic energy. It is suggested that the electron trapping processes in vitreous selenium are closely connected with the structural properties of the material. This is strongly indicated by a decrease in the shallow-trap density as the measuring temperature approaches the glass transition temperature.

I. INTRODUCTION

IN this paper, we present the results of an experimental investigation of electron trapping processes in amorphous selenium. The theoretical basis for these studies was given in the preceding paper.[1] There it was shown that under certain well-defined and experimentally realizable conditions, the equations governing the transient flow of current in an insulator with several species of traps could be solved exactly. These conditions are: (1) A small quantity of charge is injected into the insulator such that the injected space charge field produces a negligible perturbation on the externally applied electric field. (2) The time for injection is much shorter than the free-carrier transit time across the sample, so that in the absence of trapping, the current induced in the external circuit is the result of the drift motion of a thin sheet of charge along the potential gradient in the insulator. (3) Blocking electrodes are applied to the sample to prevent further injection of

* Research supported in part by the National Aeronautics and Space Administration.

† Present address: E. H. Plessett Associates, Incorporated, Santa Monica, California.

‡ This work is based in part on a thesis submitted in partial fulfillment of the requirements for the degree of Doctor of Philosophy at the University of Rochester, Rochester, New York. Present address: Department of Physics, Union College, Schenectady, New York.

[1] R. M. Blakney and H. P. Grunwald, preceding paper, Phys. Rev. **159**, 658 (1967).

charge after the thin sheet of carriers is introduced. When these conditions have been satisfied, the observed transient current pulse is here said to be in the small-signal mode, to differentiate the technique from that employing space-charge-limited injection.

The parameters in the theory are the mean free time for a free carrier between capture events T_t and the mean time-of-dwell for a carrier in a trap T_r. In principle, these quantities can be determined for each trapping species present from a single observation of the small-signal current transient, although, in practice, the method is limited to the detection of not more than two or three distinct species. If both parameters are known for a given species of trap, the capture probability and trap density can be deduced. One purpose of this report is to illustrate the application of the theory in the study of electron trapping processes in vitreous selenium.

We will discuss the trapping processes in vitreous selenium in terms of the energy-band approximation. This may be a rather poor approximation for a discussion of transport processes in view of the low value for the microscopic electron mobility which has been reported for the several modifications of selenium $\mu_0 \approx 1$ cm^2/V sec.[2–4] This value for the mobility represents a limit to the range of validity for the use of extended wave functions to describe electron-lattice interactions in solids. The self-trapping mechanism of Toyazawa[5] may be more appropriate for vitreous selenium, but neither the theory nor the energy-band structure of selenium has yet been put on a sufficiently quantitative basis to permit more than speculative discussion of our results in terms of this mechanism.

A distinguishing feature of electron transport in vitreous selenium is that the electronic drift mobility (as determined by transit time measurements) depends on temperature as $\mu_d \propto \exp(-E_m/kT)$. It has been assumed in previous work by others that the drift motion of electrons in selenium is controlled by a level of traps (hereafter designated as the m traps) variously reported at $E_m = 0.25$ eV[2] and $E_m = 0.28$ eV[3] below the conduction-band edge. (k is Boltzmann's constant and T is the absolute temperature.) We have adopted this view in the interpretation of our results, although our principal conclusions do not depend on the exact mechanism responsible for the thermally activated mobility. If the injected electrons must first be trapped into and come into equilibrium with the m traps, one might expect to see a high-current spike at sufficiently short times after injection, which would correspond to drift motion of free electrons with a microscopic mobility much larger than the trap-controlled drift mobility. Such a spike was not observed within the limit imposed by the time resolution of our apparatus, which was about 10^{-8} sec. One concludes that if the drift mobility is a trap-controlled process, the injected carriers must come into equilibrium with the m traps in a time less than 10^{-8} sec after injection. Our experiment provides no basis for supporting or questioning this hypothesis.

II. EXPERIMENTAL TECHNIQUE

The experimental arrangement was generally similar to that used by Spear[6] and others for drift mobility measurements by the transit time technique. The essential elements of the apparatus are shown schematically in Fig. 1. The sample, in the form of a thin layer of selenium, was placed between blocking electrodes, and a thin sheet of charge was injected by illuminating the sample through one (transparent) electrode with a short flash of light. Because of the high capacitance of the sample ($\sim$100 pF in our case), a direct observation of the transient current was not possible, since the unavoidably large circuit time constant distorted the current pulse. Therefore, the circuit elements were chosen to provide a time constant much greater than the transit time of the injected carriers. This resulted in a voltage signal at the input to the preamplifier which was proportional to the time integral of the current. After amplification, this signal was differentiated electronically to produce a signal proportional to the primary current in the sample. A Tektronix Type O operational amplifier was used for the differentiation and provided a sensitivity sufficient to detect currents smaller than 10^{-8} A, with a time resolution of 1 μsec.

Unsupported layers of selenium were prepared by first evaporating selenium onto aluminum foil substrates in vacuo and then separating the evaporated layers from the substrates. The adhesion of the selenium to the foil was quite low, presumably due to an inert surface layer of aluminum oxide, making the separation easy. Before mounting the sample, the unsupported

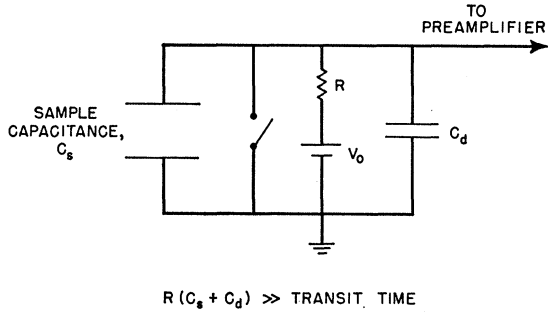

FIG. 1. Diagram of the measuring circuit. C_d is the amplifier input capacitance plus distributed capacitance; R is the parallel combination of amplifier input resistance and large resistance (8.2 MΩ) in a series with sample and battery.

[2] W. E. Spear, J. Phys. Chem. Solids **21**, 110 (1961).
[3] J. L. Hartke, Phys. Rev. **125**, 1177 (1962).
[4] J. Dresner, J. Phys. Chem. Solids **25**, 505 (1964).
[5] Y. Toyozawa, Progr. Theoret. Phys. (Kyoto) **26**, 29 (1961); J. Appl. Phys. **33**, 340 (1962).
[6] W. E. Spear, Proc. Phys. Soc. (London) **B70**, 669 (1957).

film was placed between two Pyrex films, about 1 μ in thickness, and this assembly was then clamped between the electrodes in the sample holder. The purpose of the Pyrex films was to provide the required transparent blocking layer at each electrode. The electrodes themselves were Pyrex disks coated on one side with a transparent conducting layer of tin oxide. Several other methods of sample preparation were tried before this technique was devised, all of which involved the evaporation of selenium onto rigid substrates. These proved to be unsatisfactory for measurements made over a range of temperature because the selenium tended to break up and separate from the substrate in the vicinity of 0°C.

Special high-purity (99.999+%) selenium was obtained from the American Smelting and Refining Company. Evaporation was made from alundum crucibles at a pressure of about 10^{-5} mm Hg, and the temperature of both the crucible and the substrate was monitored during evaporation. The substrate was maintained at constant temperature to within ± 2°C, and was shielded from the crucible until all the selenium had melted and reached a temperature of 320°C. This crucible temperature was maintained until all the selenium had evaporated. The initial charge of selenium was such as to produce layers about 60 μ thick.

Flash illumination of the sample was accomplished by focusing a magnified image of an air spark onto the sample. Between 10^9 and 10^{10} photons were delivered to the sample by the spark in about 10^{-8} sec over an area of about 0.25 cm^2. The total light output from the spark varied by as much as 30% between consecutive flashes, resulting in a similar variation in the magnitude of the current pulse. By the use of a quartz beam-splitter between the spark and the sample, a small fraction of the light was reflected to a photomultiplier which monitored the relative light output of each flash. This was recorded for each current transient observed. As will be shown, the magnitude of the current pulses was directly proportional to the total energy in the flash. By monitoring the flash, the current pulses could be normalized to a single flash energy, a procedure which helped to reduce the scatter in some of the data.

III. GENERAL CHARACTERISTICS OF SMALL-SIGNAL CURRENT TRANSIENTS

The appearance of the oscilloscope trace for a typical electron current transient in selenium is shown in the lower part of Fig. 2. The upper trace is the voltage pulse which was differentiated to give the lower trace. The rapid change in slope of the current trace at the center of the figure marks the transit time for the leading edge of the injected carrier distribution. Rapid electron trapping is indicated both by the shape of the current pulse prior to the transit time and the long tail thereafter. If there were no trapping, the current would be constant up to the transit time and then decrease abruptly to zero. The tail is due to the late arrival of electrons at the collecting electrode, these electrons having been captured and released one or more times by shallow traps.

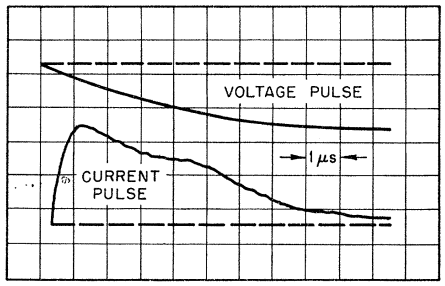

FIG. 2. Appearance of the oscilloscope trace of the voltage and current for electrons injected into a 64 μ layer of viterous selenium in the small-signal mode. The electrode area was approximately 0.25 cm^2. The top trace is the voltage signal; the bottom trace is the derivative of the voltage signal and is proportional to the small-signal transient current. The sweep speed was 1 μsec/cm for both traces and the differentiating time constant was 1 μsec. The time of collection of the injected electrons is clearly indicated by the rapid drop in the current.

It was shown in the previous paper that the magnitude of the initial current in the small-signal mode should be directly proportional to the number of photons absorbed by the sample. This is verified by Fig. 3, which shows that the linear relation holds for currents as large as 10% of the maximum current which can be passed by the sample, in agreement with the theoretical prediction. The ordinate in the figure is the initial current (before appreciable trapping occurs) normalized to the theoretical value of the trap-free, space-charge-limited current for this sample. The abscissa gives the relative

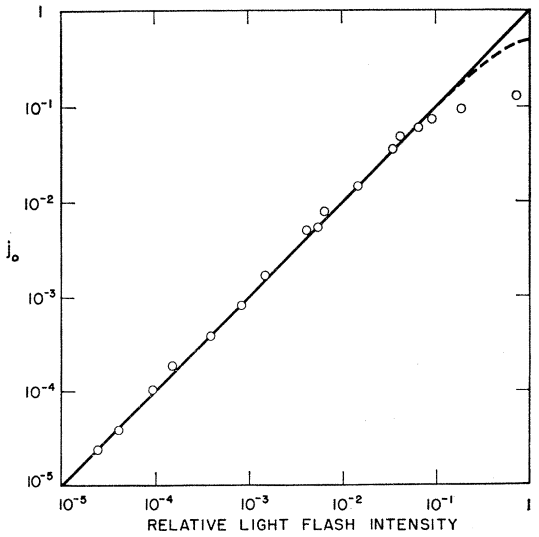

FIG. 3. Logarithm of the ratio of the initial current to the trap-free, space-charge-limited current versus the logarithm of the relative light flash intensity for one of the samples. The linear relationship is satisfied for currents as large as 10% of the maximum current which can be passed by the sample. The theoretical expression is shown as a dashed line.

energy in the light flashes which produced the transient current pulses. Because of the rapid trapping of the injected electrons, the peak of the current transient is not a good measure of the initial current, since its magnitude depends on the response time of the differentiating circuit. A better measure of this quantity is given by the initial slope of the voltage pulse, and the data for Fig. 3 were obtained by measuring this slope on voltage pulses displayed with a fast sweep speed (0.2 μsec/cm). The traces rose linearly from the base line for about 1 μsec, and when the rate of rise was corrected for the variation in spark intensity, reproducible values for the initial current were obtained.

In the mathematical analysis of the small-signal currents in insulators,[1] it was shown that the current could be expressed as a sum of terms, each of which decay exponentially with time. The number of such terms is equal to the number of distinct species of trap in the material. The electron current transients in vitreous selenium are best described in terms of two trapping species, which we shall call the s and d traps, for shallow and deep, respectively. The s traps are characterized by a high probability for thermal release of a trapped carrier in a time interval shorter than the transit time, while the probability for thermal release from a d trap is low in this same period. The expression for the transient current for this model is given by

$$J(t)=A\exp(-\alpha t)+B\exp(-\beta t), \tag{1}$$

with $\alpha+\beta=1/T_{ts}+1/T_{td}+1/T_{rs}$, $\alpha\beta=1/(T_{rs}T_{td})$,

$$\alpha A+\beta B=J_0/T_{ts}+J_0/T_{td}, \quad J_0=A+B. \tag{2}$$

In these relations, T_{ts} and T_{td} are the mean times for capture of an electron into the shallow and deep traps, respectively, T_{rs} is the mean time of dwell for an electron in an s trap, and J_0 is the initial current which flows immediately after injection and before any trapping occurs.

In Fig. 4, the logarithm of the current is plotted against time for a selenium sample in which the electric field was adjusted to give a long transit time. Under these conditions, most of the injected carriers have a chance to interact with the traps and are eventually captured into the deep traps before reaching the collecting electrode. The resolution of this curve into two exponentially decaying components is shown in the figure, along with the values for T_{ts}, T_{td}, and T_{rs}. These quantities were computed from Eqs. (2), using the values of A, B, α, and β obtained from the curve.

To demonstrate that the trapping parameters so obtained do, in fact, characterize the trapping process and can be reliably extracted from the current transients, we have replotted three current pulses in Fig. 5. These were obtained from the same sample with different voltages applied to the electrodes. All the curves have been normalized to the initial current J_0. The solid line is a plot of Eq. (1), with the constants (A,B,α, and

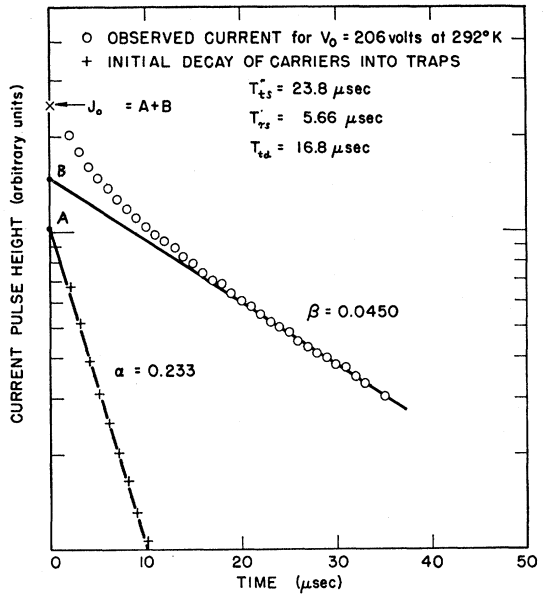

FIG. 4. The logarithm of a typical current transient is plotted as a function of time. The resolution of this curve into two exponentially decaying components is shown along with the values for T_{ts}, T_{td}, and T_{rs}.

β) obtained from an analysis of the current obtained when 300 V was applied to the sample (giving a transit time greater than 20 μsec). At this voltage, most of the carriers end up in the deep traps and never reach the collecting electrode. Since the carrier-trap interaction was allowed to go to completion, the most accurate

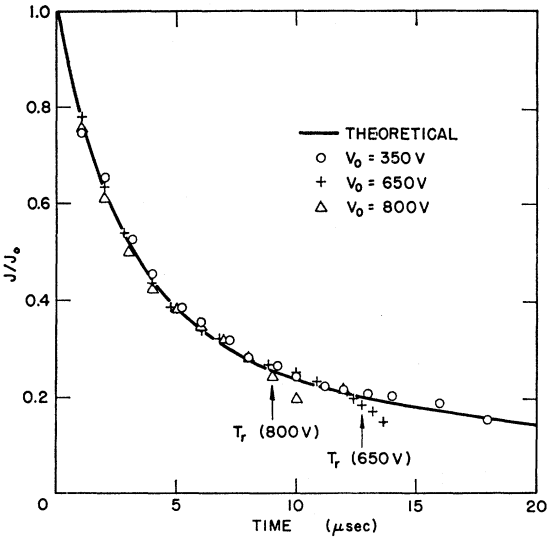

FIG. 5. Comparison of the experimental current transients in vitreous selenium with the theoretical expression. The experimental points were obtained for the same sample with different voltages applied to the electrodes. The solid line is a plot of Eq. (1), with the constants (A,B,α,β) obtained from an analysis of the current transient when 300 V was applied to the sample. The arrows indicate the approximate transit times with higher applied voltages.

values for the trapping parameters should be obtained for this case. The agreement between the theoretical prediction and the experimental curves obtained with different values of applied voltage is seen to be good.

An attempt was made to observe the decay of the injected carriers into the m traps (i.e., the traps which control the drift mobility) by examining the shape of the leading edge of the voltage pulse. By displaying the pulse with a sweep speed of 0.02 μsec/cm, an initial high rate of rise was observed, which lasted for less than 0.02 μsec, after which the slope decreased abruptly to the linear rise we have associated with the initial current. We attribute the fast initial rise to the finite duration of the flash from the spark, which is on the order of 0.02 μsec. During this period, the number of carriers in the sample which can contribute to the current is increasing. The temperature dependence of the slope of the linear portion of the voltage pulse was found to be the same as that for the drift mobility, exhibiting the same activation energy. The conclusion is that the drift motion of the electrons is controlled by the m traps for times as short as $\sim 10^{-8}$ sec after injection, so that the electrons must have come into equilibrium with these centers well before this time. Hence, our experiments can give no information about the m traps, other than their position in energy. However, the time spent by the electrons in the m traps must be taken into account if a correct interpretation is to be given of the slower trapping process.

IV. TRAPPING PROCESSES IN VITREOUS SELENIUM

The trapping parameters T_{ts} and T_{rs} for the s traps and T_{td} for the d traps were measured as a function of temperature for three samples of selenium over the range $-30°C<T<30°C$. The samples were prepared at different substrate temperatures during evaporation, but all other preparation conditions were the same. Since the qualitative behavior of the trapping parameters was found to be similar in all the samples, the data from only one of the samples will be presented in detail. The quantitative differences resulting from the different substrate temperatures during sample preparation will be discussed later. The results for one sample are shown graphically in Fig. 6, the substrate temperature in this case having been maintained at 38°C during evaporation of the selenium. Measurements of electron transit time as a function of temperature gave the activation energy for the drift mobility as $E_m=0.29$ eV, with a room-temperature (20°C) drift mobility $\mu_d=5.8\times10^{-3}$ cm^2/V sec. (All energies are referred to the conduction edge.)

Both T_{ts} and T_{td} include the time spent by the electrons in the m traps and must be corrected for this to obtain the true trapping times. The fraction of time spent by an electron in the conduction band before being captured into an s or d trap is given by $\theta_m=n_f/n_m$,

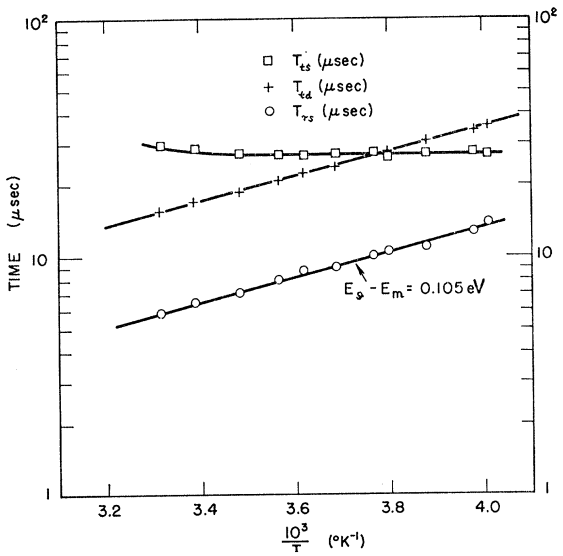

FIG. 6. The temperature dependence of the observed trapping parameters T_{ts}, T_{td}, and T_{rs} in a viterous selenium film. The substrate of this sample was maintained at 38°C during the evaporation of this sample.

where n_f is the free-carrier density and n_m is the density of carriers in the m traps. The true trapping times are, therefore, $T_{ts}'=\theta_m T_{ts}$ and $T_{td}'=\theta_m T_{td}$. In terms of the density of states in the conduction band N_c and the density of m traps N_m, θ_m may be expressed as

$$\theta_m=(N_c/N_m)\exp(-E_m/kT). \tag{3}$$

The quantity θ_m is also given by the ratio of the drift mobility to the microscopic mobility μ_0 by the relation

$$\mu_d/\mu_0=\theta_m/(1+\theta_m). \tag{4}$$

Note that if $\theta_m<1$, Eq. (4) states that the temperature dependence of θ_m should be essentially that of μ_d, i.e., $\theta_m\propto\exp(-E_m/kT)$. This assumes that μ_0 varies only slowly with temperature. Therefore, if Eqs. (3) and (4) are to be consistent, N_c/N_m cannot change rapidly with temperature.

Dressner has determined a value for the electronic mobility at room temperature by measuring the photo-Hall voltage in evaporated layers of selenium. He found $\mu=0.32\pm0.1$ cm^2/V sec. If this value is identified with the microscopic mobility, one finds $\theta_m=1.8\times10^{-2}$ at room temperature, which yields the ratio $N_c/N_m=1.9\times10^3$. With these values, the observed trapping times can now be corrected to obtain the true trapping times.

In Fig. 6, the observed trapping time for the s traps is seen to be essentially constant for temperatures below 20°C. In this time interval, the electron spends $T_{ts}'=\theta_m T_{ts}$ sec in the conduction band from which it can be captured by an s trap. The capture probability C_s associated with these traps is given by $C_s=(N_s T_{ts}')^{-1}$, with N_s being the density of the s traps. On substituting for T_{ts}' into this expression and using Eq. (3) for θ_m,

the capture probability becomes

$$C_s = N_m/(N_c N_s T_{ts}) \exp(E_m/kT). \quad (5)$$

If one makes the reasonable assumption that the mean free time between m-trapping events is not strongly temperature-dependent, and also assumes that N_s is independent of temperature, the observed constancy of T_{ts} (Fig. 6) implies that the capture probability for the s traps increases exponentially as the temperature decreases, with a characteristic energy equal to the activation energy for the drift mobility.

The activation energy for the s traps can be determined from the temperature dependence of T_{rs} in Fig. 6, noting that $1/T_{rs}$ is the rate constant for thermal emptying of these centers. If n_s is the density of electrons in the s level, the principle of detailed balance in the steady states that $n_s/T_{rs} = n_f/T_{ts}'$, and this leads to

$$1/T_{rs} = N_c/(N_s T_{ts}') \exp(-E_s/kT), \quad (6)$$

where E_s is the depth of the shallow trap below the conduction band. On substituting $T_{ts}' = \theta_m T_{ts}$ and using Eq. (3) for θ_m, one obtains

$$T_{rs} = (N_s T_{ts})/N_m \exp[(E_s - E_m)/kT]. \quad (7)$$

From Fig. 6, the value of $E_s - E_m$ is found to be 0.10 eV, and since $E_m = 0.29$ eV, this places the s level at 0.39 eV below the conduction-band edge. The pre-exponential factor in Eq. (7) yields the ratio of trap densities, $N_s/N_m = 4.6\times10^{-3}$. On using the previous result for N_c/N_m, the ratio of the shallow-trap density to the density of states in the conduction band in $N_s/N_c = 2.4\times10^{-6}$.

For the deep level, only the trapping time T_{td} could be determined and this is seen in Fig. 6 to increase exponentially with $1/T$ with a characteristic energy of

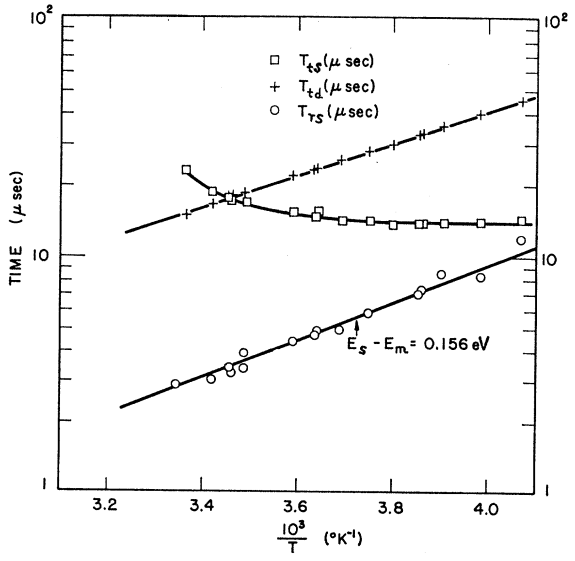

FIG. 7. Same as Fig. 6, except the substrate of this sample was maintained at 48°C during the evaporation of this film.

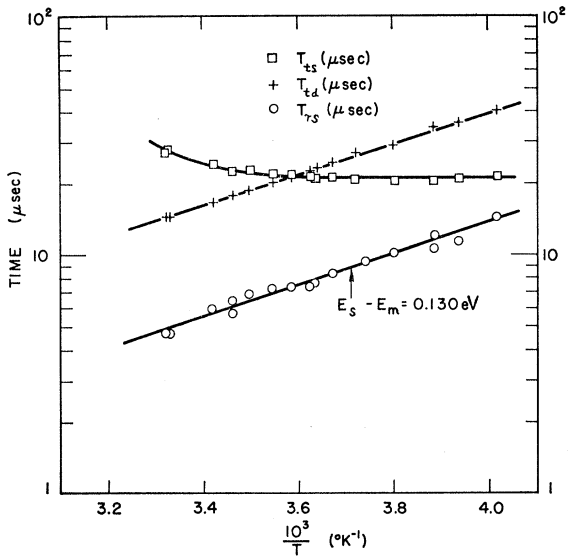

FIG. 8. Same as Fig. 6, except the substrate of this sample was maintained at 58°C during the evaporation of this film.

$E_d' = 0.1$ eV. If it is again assumed that the density of the d states does not depend on temperature, the capture probability for these traps may be expressed in the form of Eq. (5) with a characteristic energy $E_m - E_d' = 0.19$ eV.

The results for the three films investigated in detail are presented graphically in Figs. 6, 7, and 8, and summarized in Table I. As indicated above, these samples were prepared with the substrates at different temperatures during the evaporation of the selenium. For all the films, the measured value of T_{ts} was constant in the temperature range below 0°C. With sample No. 3 (58°C substrate temperature, Fig. 8), T_{ts} increased at temperatures above 0°C, becoming almost double its low-temperature (constant) value at about 25°C. A similar but smaller increase is seen to occur with sample No. 3 (Fig. 7), beginning at about 15°C. The changes in T_{ts} were reversible over the temperature range used in these experiments, and the values were reproducible as the temperature was cycled from low to high and back to low.

Examination of Table I shows some interesting trends. The activation energy for the electronic drift mobility is higher and the density of the m traps is lower, the

TABLE I. Experimental results for the three selenium film samples.

Sample Temperature of substrate in preparation	No. 1 38°C	No. 2 48°C	No. 3 58°C
μ_d(0°C) cm²/V sec	2.4×10^{-3}	2.4×10^{-3}	1.7×10^{-3}
E_m eV	0.29	0.31	0.33
θ_m(0°C)	7.5×10^{-3}	7.5×10^{-3}	5.3×10^{-3}
N_m/N_c	5.2×10^{-4}	2.4×10^{-4}	1.4×10^{-4}
E_s eV	0.39	0.44	0.48
N_s/N_c	2.4×10^{-6}	3.6×10^{-7}	6.0×10^{-8}
$N_c C_s$(0°C) sec⁻¹	2.7×10^{12}	1.7×10^{13}	2.3×10^{14}
$(E_m - E_d')$ eV	0.19	0.18	0.19

higher the temperature of the substrate during sample preparation. This behavior of E_m has been examined in detail for several films by a careful measurement of the temperature dependence of the drift mobility. It was found that E_m increased linearly with sample preparation temperature from 0.25 eV for room-temperature evaporation, as reported by Spear, to 0.33 eV for the film prepared at 58°C. Concurrently, the m-trap density (N_m/N_c) decreased by a factor of about 4 over this range. This behavior is reflected in Table I. A second trend worth noting is the rapid decrease in the shallow-trap density as the sample preparation temperature was increased. This is largely compensated by an increase in the capture probability, so that the true shallow-trapping time does not vary by more than a factor of 2 in the three samples.

The main results of these experiments may be summarized as follows: (1) Electron-trapping processes in vitreous selenium involve three distinct species of trap. Two of these (those which control the drift mobility and the deep traps) have been recognized previously. These experiments have shown that there is a third level (s traps), distinguished here for the first time, lying between the other two levels and which acts as a shallow-trapping level in the sense defined above. (2) The density of these states is less than that of the m states by a factor of 10^{-2}–10^{-3}. (3) The energy separation of the s level from both the conduction-band edge and the m level depends on the sample preparation temperature, the separation increasing as this temperature is increased. (4) The capture probability of both the s and d traps increases exponentially with $1/T$ with a characteristic energy. (5) At sufficiently low temperature, the shallow-trap density is independent of the temperature of measurement but tends to decrease rapidly as the measuring temperature is increased beyond a critical value. This critical temperature depends on the temperature at which the sample was prepared. This is a reversible effect.

Comparison of our results with previous measurements made by Hartke[3] and Spear[6] is difficult for the following reasons: (1) We have shown that the density and energy depth of the m and s traps depend on the temperature of the substrate during sample preparation. Previous investigators only estimated this temperature. (2) Measurements on the mean free drift time for electrons have been made by Hartke.[3] His results are based on an analysis which is valid when only deep trapping occurs; that is, no thermal release of the trapped carriers occurs during the time of the experiment. This we believe is not a valid assumption.

Realizing the above limitations, a quantitative comparison can be made: (1) Spear[6] determined the ratio $N_m/N_c \approx 1.6\times10^{-3}$, while Hartke[3] obtained $N_m/N_c \approx 4\times10^{-5}$. Here we have taken the liberty of recalculating Spear's and Hartke's results using $\mu_0=0.32$ cm²/V-sec as measured by Dressner.[4] These ratios are in good agreement with the values given in Table I. (2) Hartke found that the mean time for capture of an electron into a deep trap is strongly temperature-dependent. This result is in agreement with our results as shown in Figs. 6, 7, and 8.

V. DISCUSSION

Our results on electron trapping processes in amorphous selenium suggest that the traps we have observed are closely connected with the structural properties of the material. It seems unlikely that impurities are responsible for either the m or s traps for the following reasons: (1) The density and energy depth of both sets of traps has been shown to depend on the conditions existing during sample preparation particularly in the temperature of the substrate during sample preparation. (2) The density of the s traps changes in a reversible way above a critical temperature of measurement (below which it is constant) which depends on the sample preparation conditions. (3) The exponential increase of the capture probability with $1/T$ for both the s and d levels is not suggestive of trapping by impurities. In view of these observations, it seems to us that the traps are associated primarily with the structure of amorphous selenium.

Brieglieb[7] has estimated the relative proportion of Se_6 rings and many-membered chains in selenium samples prepared by vacuum evaporation onto substrates held at various temperatures. The two components were distinguished by the difference in their solubility in CS_2. He found that the proportion of selenium chains increased at the expense of rings as the temperature of the substrate during film preparation was increased. X-ray studies by Richter and Herre[8] have indicated that the atomic distribution in samples prepared at the temperature of liquid N_2 were essentially different from that in films prepared at room temperature. In the latter case, small regions of hexagonal symmetry were observed which Richter and Herre attributed to the presence of many-membered chains, while in the former case there was a preponderance of ring formation.

Eisenberg and Tobolsky[9] have calculated the degree of chain polymerization in amorphous selenium as a function of temperature and predict a maximum polymerization at a temperature well below the melting point. They argued that the behavior of selenium should be qualitatively similar to that of sulphur, which exhibits a maximum degree of polymerization above the melting point (as manifested by a maximum in the viscosity-versus-temperature curve). On the basis of the chemical thermodynamic properties of selenium, the same formalism was applied to selenium to predict that the maximum chain length should occur in the neighbor-

[7] G. Brieglieb, Z. Physik Chem. (Leipzig) **A144**, 321 (1929).
[8] H. Richter and F. Herre, Z. Naturforsch. **13a**, 874 (1959).
[9] A. Eisenberg and A. Tobolsky, J. Polymer Sci. **46**, 19 (1960).

hood of 83°C. Below this temperature, the chain length decreased rapidly until approximately 310°K according to this model, thereafter decreasing more slowly. This calculation predicts that the average chain length should decrease by about an order of magnitude as the temperature goes from 331°K (58°C) to 311°K(38°C). In Table I, the shallow-trap density is seen to be greater by a factor of 40 in the sample prepared at 38°C over that prepared at 58°C. This suggests that the shallow traps are associated with the ends of chains, the length distribution of which is characteristic of the sample preparation temperature and is "frozen-in" at the temperature at which the measurements were made.

Amorphous selenium has many of the characteristics of a glass. In particular, selenium exhibits a glass transition temperature which may be associated with a second-order transition. For example, the slopes of the volume and entropy-temperature curves suffer a sharp decrease with decreasing temperature at the glass transition temperature T_g. For $T>T_g$, amorphous selenium is considered to be supercooled liquid, while for $T<T_g$, it is a glass. Eisenberg has determined $T_g=31.0$°C for selenium for a study of its visco-elastic properties.

The physics of the glass transition is not completely understood, but it is generally thought to involve a rapid change in the number of configurations available to the components of the glass (in this case, the selenium chain molecules). As the temperature decreases through T_g, the number of available configurations for the molecules should decrease abruptly. Hence, if a sample prepared at a temperature $T_1>T_g$ is rapidly cooled below T_g, we would expect the chain-length distribution in the quenched sample to resemble closely that corresponding to the temperature T_1. Our samples were cooled to room temperature in a matter of a few minutes after the completion of the evaporation, and all trapping measurements were made at temperatures $T<T_g$.

The decrease in shallow-trap density as the measuring temperature approaches the glass transition temperature may be understood in terms of the linking of chains. This shows up as an increase in the observed trapping time in Figs. 6, 7 and 8. As the temperature was raised, an increasing number of configurational degrees of freedom became available to the chain ends, improving the chances for linking up. This is to be expected from the increase in polymerization predicted by Eisenberg and the experimental observations of Briegleb and Richter and Herre.

PHYSICAL REVIEW VOLUME 159, NUMBER 3 15 JULY 1967

Dynamics of Radiation Damage in Face-Centered-Cubic Alkali Halides

IAN McC. TORRENS AND LEWIS T. CHADDERTON
North American Aviation Science Center, Thousand Oaks, California
(Received 1 March 1967)

Computer simulations of ionic motion in 3-dimensional potassium chloride and sodium chloride crystallites have been undertaken to investigate the effect of the regular lattice in influencing the energy spread in the crystal from a primary event such as might be caused by an incident energetic charged particle. Focusing of energy has been found to occur in several low-index crystallographic directions, including those where successive collisions involve oppositely charged ions. The neighboring assisting lines of ions exert considerable influence on the rate of energy loss along the focusing line, on the solid angle in which focusing occurs, and on the threshold energy for permanent ionic displacement from a lattice site, which was found to be a minimum of 25–30 eV in the ⟨110⟩ directions of potassium chloride. The feasibility of some mechanisms of F-center formation through ionic displacement is discussed in the light of this value of displacement threshold. The computations reveal a new concept of focusing, for which there is a *lower* energy limit for propagation of a focuson. This limit can be as high as several hundred electron volts for higher-order focusing through asymmetric assisting ionic "lenses." At energies above the lower focusing-energy limit, the momentum transfer of the moving ion to its neighbors between focusing collisions is sufficiently small compared to its forward momentum for its trajectory to be altered only slightly by collision with different parts of the assisting lens. At lower energies, asymmetric collisions with lens ions result in defocusing.

I. INTRODUCTION

IN the past few years the influences of the crystal lattice on the motion of energetic charged particles and on the dissipation of energy in a crystalline material during irradiation have become topics of major interest to investigators of radiation damage in the solid state. Anisotropy of the lattice has the effect of enhancing the processes of energy transfer in some crystalline directions over that which we might expect if the atoms of the irradiated material were randomly distributed in the solid. An important example of this is the phenomenon of *focusing*,[1,2] in which energy is transferred

[1] R. H. Silsbee, J. Appl. Phys. **28**, 1246 (1957).
[2] M. W. Thompson and R. S. Nelson, Proc. Roy. Soc. (London) **A259**, 458 (1961).